Published in final edited form as:
Phys Rev E Stat Nonlin Soft Matter Phys. 2011 May ; 83(5 Pt 1): 051925.

Measurement of the nonlinear elasticity of red blood cell membranes

YongKeun Park[1,2,8], **Catherine A. Best**[3], **Tatiana Kuriabova**[4], **Mark L. Henle**[5], **Michael S. Feld**[1], **Alex J. Levine**[6], and **Gabriel Popescu**[7,*]

[1]G. R. Harrison Spectroscopy Laboratory, Massachusetts Institute of Technology, Cambridge, MA 02139

[2]Harvard-MIT Division of Health Science and Technology, Massachusetts Institute of Technology, Cambridge, MA 02139, USA

[3]College of Medicine, University of Illinois at Urbana-Champaign, Urbana, IL 61801

[4]Department of Physics, University of Colorado, Boulder, CO 80309

[5]School of Engineering and Applied Sciences, Harvard University, MA 02138

[6]Department of Chemistry & Biochemistry, UCLA, CA 90095

[7]Quantitative Light Imaging Laboratory, Department of Electrical and Computer Engineering, Beckman Institute for Advanced Science & Technology, University of Illinois at Urbana-Champaign, Urbana, IL 61801

Abstract

The membranes of human red blood cells (RBCs) are a composite of a fluid lipid bilayer and a triangular network of semiflexible filaments (spectrin). We perform cellular microrheology using the dynamic membrane fluctuations of the RBCs to extract the elastic moduli of this composite membrane. By applying known osmotic stresses we measure the changes in the elastic constants under imposed strain and thereby determine the nonlinear elastic properties of the membrane. We find that the elastic nonlinearities of the shear modulus in tensed RBC membranes can be well-understood in terms of a simple worm-like chain model. Our results show that the elasticity of the spectrin network can mostly account for the area compression modulus at physiological osmolality, suggesting that the lipid bilayer has significant excess area. As the cell swells, the elastic contribution from the now tensed lipid membrane becomes dominant.

I. Introduction

Blood serum is typically maintained at fixed osmolality to control the flux of water to the circulating RBCs. When placed in hypotonic solutions (i.e., solutions with a lower concentration of solutes), the hemoglobin (Hb)-rich interior of the RBCs draws water into the cells, causing swelling and, in extreme cases, bursting. Alternatively, RBCs shrink when placed in hypertonic solutions, as the osmotic pressure difference forces water out of the cytosol of the RBCs.

*gpopescu@illinois.edu.
[8]Current address: Department of Physics, Korea Advanced Institute of Science and Technology, Daejeon 305-701, Republic of Korea

PACS: 87.16.D- Membranes, bilayers, and vesicles; 87.16.dj Dynamics and fluctuations; 87.16.dm Mechanical properties and rheology; 83.60.Df Nonlinear viscoelasticity

In addition to changing the cells' morphology, these volume changes driven by osmotic pressure variations modify the mechanics of the cells. Measurements of the mechanical properties at various fixed osmotic pressures thus allow one access to the nonlinear elasticity of the cells. Since RBCs do not have an internal cytoskeleton or other complex sub-cellular organelles, their mechanics is determined entirely by their membrane, which is a lipid bilayer coupled to a triangular lattice of semiflexible polymer filaments mainly composed of spectrin. Any observed change in the mechanics of the cells under osmotic stress must reflect the elastic nonlinearity of this composite membrane as it is tensed or relaxed by the influx or respectively efflux of water. Thus, the ability to measure the *linear response* properties of the cell membrane at varying states of osmotic stress allows one to experimentally probe the *nonlinear elastic response* of this tethered membrane.

In this paper we report on a series of microrheological measurements of RBC membrane mechanics obtained at varying levels of osmotic stress. We simultaneously measure the cellular volume so that we may quantitatively measure the change in the elastic properties of the composite membrane as a function of applied strain. Our results provide insight into the general problem of the nonlinear mechanics of tethered membranes but also have biological implications for understanding the effects of blood serum osmolality on RBC mechanics. Since these cells undergo large deformations and significant changes in osmotic stress in the microvasculature, understanding the nonlinear mechanics of RBCs under osmotic pressure may have direct physiological implications.

II. Model and methods

The RBC plasma membrane is a 4–5 nm thick fluid lipid bilayer mechanically characterized by a bending modulus κ and an area compression modulus K_A. On the cytoplasmic or interior side of the membrane there is the triangular spectrin network with mesh size of 90 nm that is anchored to the bilayer via transmembrane proteins at the nodes of this cross-linked network [1]. On length scales long compared to the lattice constant, the mechanics of this network can be described as a two-dimensional elastic continuum having two equal Lamé constants $\mu=\lambda$. Given the viscosity of the fluid lipid bilayer, viscous stresses in the membrane are subdominant up to frequencies of ~10^3 Hz [2]. The cytosol of the RBC consists mainly of a spatially homogenous Hb solution of viscosity η_c that, due to the high Hb concentration, is significantly more viscous than that of the surrounding solvent: $\eta_s<\eta_c$. Thus, the mechanical description of the RBC contains four parameters: κ, K_A, μ, η_c. Of these, κ is thought to depend solely on the lipid composition of the bilayer, K_A depends on a combination of the bilayer's surface tension and the area modulus of the underlying spectrin network, and μ depends solely on the shear modulus of that network. Finally, while the viscosity of the surrounding solvent is known, the viscosity of the highly concentrated cytosol solution η_c will vary strongly with Hb concentration and thus with osmotic pressure.

A number of techniques have been used to obtain quantitative information about mechanics of live RBCs, including pipette aspiration [3], electric field deformation [4], magnetic beads cytometry [5] and optical tweezers [6, 7]. However, none of these methods can probe all of the mechanical parameters of the RBC membrane simultaneously. Moreover, these approaches require contact by an external probe and operate with a large force (or deformation) that may invalidate the assumption of linear response. Fluctuations in RBC membranes are intrinsic reporters of the linear mechanical response; they offer a non-perturbing window into the structure, dynamics, and function of the intact cell [8–13]. In order to measure the nanoscale membrane fluctuations with high accuracy and low noise, we employed diffraction phase microscopy (DPM) [14], which has been used successfully for imaging cell structures and dynamics [15–19]. Analyzing the observed fluctuation spectrum of a soft elastic object to determine its (visco-)elastic properties is commonly referred to as

microrheology [20, 21]. The analysis of the fluctuation data requires (i) a model of the frequency-dependent linear response to applied forces, and (ii) an assumption of thermal equilibrium. Using the latter assumption and the Fluctuation-Dissipation Theorem [22], one may fit a model of the response function containing the appropriate elastic moduli to the observed fluctuations. For the case in question, we use a dynamical model of the undulations of a spherical shell separating Newtonian fluids of differing viscosities [23]. The assumption of thermal equilibrium is approximate. It is known that ATP-dependent fluctuations exist in RBC membranes. However, these nonthermal forces are subdominant; the nonthermal contributions to the fluctuations appear to be confined principally to changes in the area compression modulus [17]. There is little effect on the shear and bending moduli of the membrane.

In this study we use cellular microrheology to probe the effective linear elastic response of the membrane at varying states of stress, controlled by an external osmotic pressure. To modulate the osmolality of the medium, we prepared RBC suspensions (10^6 cell/μl) with eleven different osmolalities ranging from 100 to 600 mOsm/kg H_2O. We followed the standard protocols for RBC preparation [11]. Fresh blood samples were collected and diluted 1:5 in Hank's buffer saline solution (HBSS) and then immediately centrifuged at 2000 g at 5°C for 10 minutes to separate RBCs from plasma. The RBCs were washed three times and then resuspended in the given NaCl solutions. The NaCl solutions contained increasing concentrations of NaCl (0.3–1.8) %, which correspond to suspension osmolalities ranging from 100–600 mOsm/kg. Using DPM we extracted quantitative optical phase shifts $\varphi(x,y,t)$ associated with the cells, at spatial and temporal resolutions of nm and ms, respectively [14, 16]. The cell thickness profile is obtained from the optical phase shift as $h(x,y,t)=(\lambda/2\pi\Delta n)\varphi(x,y,t)$. Since the refractive index difference, Δn, is mainly contributed from homogeneous Hb solution in cytoplasm, the integration of optical phase shifts over cell area, i.e. the dry mass [24], is related to the volume of RBC as, $Volume=\int\langle h(x,y)\rangle dA$. The Δn was calculated using the RBC volume data in the literature [25].

III. Results and discussions

A. Topography and membrane fluctuations of RBCs at different osmotic pressure

Thickness profiles and horizontal cross-sections of RBCs in hypotonic, isotonic, and hypertonic media are shown in Fig. 1. It is clear that different osmolalities of the extracellular medium result in significant changes in RBC shape. In a hypotonic medium (100 mOsm/kg, Fig. 1a), RBCs are swollen due to water influx but still maintain the dimpled region in the center. At the osmotic pressure less than 100 mOsm/kg, most of RBCs are lysed. In the hypertonic case (600 mOsm/kg, Fig. 1c), RBCs shrink due to water efflux. In a hypertonic medium, the projected area of the membrane is lower than that of normal RBCs, which is indicative of an increase in the membrane tension caused by cell swelling; see Fig. 2a. In contrast, the projected area in a hypertonic medium does not change significantly. We extracted the mean corpuscular hemoglobin (MCH), i.e., the total amount of Hb in the cell, as the product of the Hb concentration and cytoplasmic volume. The Hb concentration was retrieved using its known relationship with the refractive index [26]. MCH maintains constant values at different osmolalities (Fig. 2c), which is consistent with the impermeability of the RBC membrane to large Hb proteins.

The membrane fluctuations were obtained by subtracting the time-averaged cell profile from each instantaneous topography map in the series, $\Delta h(x,y,t) = h(x,y,t)-\langle h(x,y)\rangle$. The root mean squared (RMS) displacement of membrane fluctuations, $\sqrt{\langle\Delta h^2\rangle}$, shows that the maximum membrane fluctuations occur around 300 mOsm/kg, which is within the normal physiological blood osmolality (Fig. 2d). The decreased deformability of RBCs in both hypo- and hypertonic conditions is consistent with a variety of experimental techniques

including laser scattering, cell elongation measurements, and blood filtration experiments [27, 28].

B. Mechanical properties of RBCs at different osmotic pressure

In order to investigate the mechanical properties of RBCs, we analyze the spatial correlations of the out-of-plane membrane fluctuations using a continuum model of the composite spectrin-network/lipid membrane [29]. Our recent theoretical description incorporates the coupling between the bending and compression modes of the curved membrane [29] and allows us to determine quantitatively the cell's mechanical parameters: κ, K_A, μ, η_c. The details of the model have been discussed elsewhere [23, 29, 30]. The two-point correlation function of the membrane fluctuations was calculated as $C(d, t)=\langle \Delta h(d, t)\Delta h(0,0)\rangle$, where the angular brackets denote both spatial and temporal averaging. As shown in Fig. 3, the theoretical model provides a very good description of the experimental data, which allows us to extract the cell material properties. In addition, we find that there is generically a single best fit, since the bending modulus controls the high wavenumber features of the correlation function while the other elastic constants dominate the lower wavenumber features. To obtain these fits to $\tilde{C}(d,\omega)$, we adjust the following parameters: the shear μ and area compression K_A moduli of the spectrin network and lipid bilayer, the bending modulus κ of the lipid bilayer, the viscosity of the cytosol η_c and the radius of the sphere R. We constrain our fits by setting R to the average radius of curvature of the RBC obtained directly from the data and fixing the viscosity for extracellular medium to be η_s =1.2 mPa·s [31]. Furthermore, we assume that the elastic properties of composite membrane are dominated by reactive (i.e. non-dissipative) terms, so that we may treat the elastic constants as real and frequency-independent. This assumption is supported *a posteriori* by our making fits to correlation functions at two frequencies separated by a factor of ~ 8 with the same elastic parameters. This leaves a four dimensional space of fitting parameters spanned by κ, K_A, μ, and η_c. For a triangular elastic network we expect $\mu=\lambda$ [32] so positive values of dimensionless parameter $\delta= K_A\mu-2$ measures the importance of the contribution of the lipid bilayer's surface tension to the effective area compression modulus of the composite membrane.

From these fits we determined the three mechanical properties of RBC membrane at different osmolalities (Fig. 4). We also extracted the viscosity of the cytosol by fitting the fluctuation data at two frequencies; the viscosity generates the only frequency-dependent stress. The shear modulus of spectrin network μ in hypotonic media shows a significant increase compared to the normal and hypertonic cases. Interestingly, μ does not change above 300 mOsm/kg. As expected, the spectrin network becomes significantly less compliant ($\mu \approx 13\ \mu\mathrm{Nm}^{-1}$) under tension. We model the spectrin network as a perfect triangular lattice of semiflexible worm-like chain (WLC) filaments, using a standard value for the thermal persistence length of spectrin l_p=7.5nm At physiological osmolality (300 mOsm/kg), we can account for the observed shear modulus using a standard value for the lattice constant of the spectrin network at physiological osmolality a_0= 90 nm and assuming that the spectrin contour length between nodes of the network is L = 170 nm, which is close to previous measurements [31]. We now assume that lower osmolality leads to a uniform extension of the spectrin lattice constant: $a(V)= a_0\ (V/V_0)^{1/3}$, where V_0 is the volume of the cell at physiological osmolality and V is the measured volume under osmotic stress. From this extension of the lattice and the WLC model [33] we determine the effective spring constant of the stretched spectrin in the osmotically stressed cells, which allows predictions of the RBC shear modulus without additional fitting parameters. The results fit the observed increase in the shear modulus remarkably well. There is some uncertainty in the reported values of l_p with values ranging from 6 to 10 nm [34, 35]. To investigate this we changed l_p in our fits and simultaneously adjusted L to obtain the measured value of μ at 300 mOsm/

kg. We then determined which of these solutions were consistent with our data for stretched networks (in hypertonic media). We find that our data is consistent with 7 nm < l_p < 9 nm using L ranging from 173 nm to 163 nm respectively.

The values of K_A at physiological osmolality (18–20 μN/m) are in agreement with previous measurements based on membrane fluctuations which reported area compression moduli in the range of 1–10 μN/m [10, 12]. We note that the measured K_A are lower than the previous values measured by micropipette aspiration technique which are in the range of 300–500 mN/m [25]. The apparent inconsistency between the difference experiments can be understood by noting that there is strong strain stiffening in the membrane as the membrane fluctuations are removed by an applied tension in micropipette aspiration technique. This is indeed evident in our data; the area compression modulus K_A also increases up to 50 μN/m as the membrane is tensed by the osmotic stress (Fig. 4a). Returning to our measure of δ to assess the relative contributions of spectrin network and lipid bilayer to K_A, we find that for physiological osmolalities (300mOsm/kg) $\delta \cong 0.1$, showing that the spectrin network is the dominant contributor to the area modulus and implying that there is significant excess area in the membrane. As the cell is swollen, we find that δ increases monotonically to ≅ 2.2, consistent with a dramatic reduction in the excess area and the dominance of the lipid bilayer's tension in determining K_A.

The membrane bending modulus, on the other hand, does not show a significant dependence on osmolalities ($\kappa \approx 5\ k_BT$). This indicates that the composition of the RBC bilayer does not change with osmotic stress. The values for measured κ are in agreement with the previously reported values in the range of 3–7 k_BT which were measured from membrane fluctuations [8, 36]. However, micropipette techniques [37] and the analysis of RBC membrane fluctuations at one point on the edge of visible cell [12, 13] both report a bending modulus of ~50 k_BT. In the former case, we suggest the higher value may be attributed to elastic nonlinearities. In the latter case, the higher curvature of the RBC membrane at the edge may effectively suppress fluctuations rendered a higher measured value.

Finally, the viscosity of the cytosol η_c increases monotonically with increasing osmolality since water leaves the cell (through aquaporin-1 channels) increasing the cytoplasmic Hb concentration, resulting in an increase of cytosolic viscosity [38]. We speculate that large changes in the cytosolic viscosity may have a physiologically protective effect. By increasing viscous dissipation when RBCs pass through the small capillaries of the kidney, where the osmolality can be as high as 1200 mOsm/kg, the viscous stresses in cytosol may reduce in-plane membrane stresses and prevent cell lysis as they undergo large-scale deformation.

IV. Summary and conclusions

In summary, we have used the dynamic fluctuations of RBCs under varying osmotic stress to measure the nonlinear response of the composite membrane's shear modulus, bending modulus, and area compression modulus. By examining data at different frequencies we also obtain the cytosolic viscosity. We find that the composite membrane is strongly strain hardening under tension in both shear and area moduli. The shear modulus enhancement is easily understood in terms of the WLC model. Further work is needed to understand the nonlinear stiffening of K_A under tension. Previous measurements of RBC mechanics report two sets of elastic moduli separated by about four orders of magnitude. Fluctuation data are consistent with our smaller measurements, while micropipette aspiration techniques consistently report the larger values. We propose that consideration of the nonlinear mechanics of the membrane may resolve much of this discrepancy. Detailed measurements

of precisely those elastic nonlinearities, such as reported here, are the key route to testing this proposal.

As expected, the bending modulus is highly insensitive to imposed osmotic stress and the cytosolic viscosity increases with Hb concentration. These elastic constants are all relatively insensitive to membrane relaxation in hypertonic solutions. Understanding this point may require more sophisticated models that include steric interactions between parts of the membrane. Finally, we note that the RBC moduli reach their minimal values at physiological osmolality, perhaps reflecting some evolutionary tuning of these elastic nonlinearities.

Acknowledgments

This research was supported by the National Institutes of Health (P41-RR02594 18-24). G.P. was partially supported by the National Science Foundation (08-46660 CAREER), National Cancer Institute (R21 CA147967-01). A.J.L. acknowledges partial support from NSF-DMR-0907212. The authors acknowledge Hawoong Jung and Kyomin Jung, Korean Advanced Institute of Science and Technology for statistical analysis, and Ramachandra R. Dasari, Massachusetts Institute of Technology, for fruitful discussions. YKP and GP deeply appreciate the guidance and advice from the late Prof. Michael S. Feld.

References

1. Discher DE, Carl P. Cell Mol Biol Lett. 2001; 6:593. [PubMed: 11598637]
2. Cicuta P, Keller SL, Veatch SL. J Phys Chem B. 2007; 111:3328. [PubMed: 17388499]
3. Discher DE, Mohandas N, Evans EA. Science. 1994; 266:1032. [PubMed: 7973655]
4. Engelhardt H, Gaub H, Sackmann E. Nature. 1984; 307:378. [PubMed: 6694733]
5. Puig-de-Morales-Marinkovic M, et al. Am J Physiol Cell Physiol. 2007; 293:C597. [PubMed: 17428838]
6. Dao M, Lim CT, Suresh S. J Mech Phys Solids. 2003; 51:2259.
7. Sleep J, et al. Biophys J. 1999; 77:3085. [PubMed: 10585930]
8. Brochard F, Lennon JF. J Physique. 1975; 36:1035.
9. Boal DH, Seifert U, Zilker A. Phys Rev Lett. 1992; 69:3405. [PubMed: 10046810]
10. Gov N, Zilman AG, Safran S. Phys Rev Lett. 2003; 90:228101. [PubMed: 12857343]
11. Popescu G, et al. Phys Rev Lett. 2006; 97:218101. [PubMed: 17155774]
12. Betz T, et al. Proc Natl Acad Sci U S A. 2009; 106:15312.
13. Yoon Y, et al. Biophys J. 2009; 97:1606. [PubMed: 19751665]
14. Popescu G, et al. Opt Lett. 2006; 31:775. [PubMed: 16544620]
15. Popescu, G. Methods in Cell Biology. Jena, BP., editor. Elsevier; 2008.
16. Park YK, et al. Proc Natl Acad Sci USA. 2008; 105:13730. [PubMed: 18772382]
17. Park YK, et al. Proc Nat Acad Sci. 2010; 107:1289. [PubMed: 20080583]
18. Mir M, et al. Opt Exp. 2009; 17:2579.
19. Ding H, et al. Phys Rev Lett. 2008; 101:238102. [PubMed: 19113597]
20. Mason TG, Weitz DA. Phys Rev Lett. 1995; 74:1250. [PubMed: 10058972]
21. Levine A, Lubensky T. Physical Review Letters. 2000; 85:1774. [PubMed: 10970611]
22. Chaikin, PM.; Lubensky, TC. Principles of Condensed Matter Physics. Cambridge University Press; 1995.
23. Park YK, et al. Proc Nat Acad Sci. 2010
24. Popescu G, et al. Am J Physiol: Cell Physiol. 2008; 295:C538. [PubMed: 18562484]
25. Evans E, Fung YC. Microvasc Res. 1972; 4:335. [PubMed: 4635577]
26. Friebel M, Meinke M. Applied optics. 2006; 45:2838. [PubMed: 16633438]
27. Schmid-SchoNbein H, Wells ROE, Goldstone J. Circ Res. 1969; 25:131. [PubMed: 5806159]
28. Mohandas N, et al. Journal of Clinical Investigation. 1980; 66:563. [PubMed: 6156955]

29. Kuriabova T, Levine AJ. Physical Review E. 2008; 77
30. Milner S, Safran S. Physical Review A. 1987; 36:4371. [PubMed: 9899393]
31. Hochmuth RM, Buxbaum KL, Evans EA. Biophys J. 1980; 29:177. [PubMed: 7260246]
32. Feng S, Sen PN. Phys Rev B. 1984; 52:216.
33. Bouchiat C, et al. Biophys J. 1999; 76:409. [PubMed: 9876152]
34. Stokke B, Mikkelsen A, Elgsaeter A. Biochimica et Biophysica Acta (BBA)-Biomembranes. 1985; 816:102.
35. Svoboda K, et al. Biophys J. 1992; 63:784. [PubMed: 1420914]
36. Zilker A, Ziegler M, Sackmann E. Phys Rev A. 1992; 46:7998. [PubMed: 9908150]
37. Evans E. Biophys J. 1983; 43:27. [PubMed: 6882860]
38. Wells R, Schmid-Schonbein H. Journal of Applied Physiology. 1969; 27:213. [PubMed: 5796309]

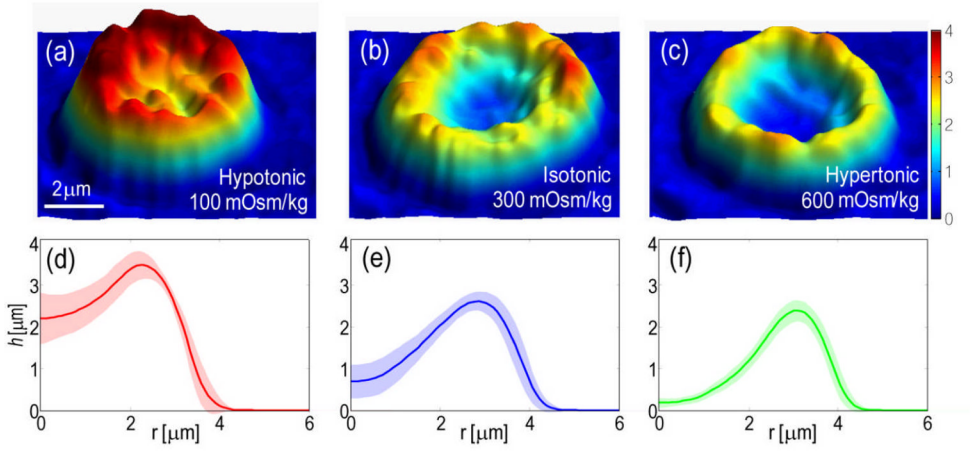

FIG. 1.

(a–c), Topography of a RBC exposed to hypotonic (a), isotonic (b), and hypertonic (c) solutions. (d–f), Corresponding membrane height as a function of a distance from the center of cells. Thick lines show the average values and the shaded areas represent standard deviations for 20 RBCs.

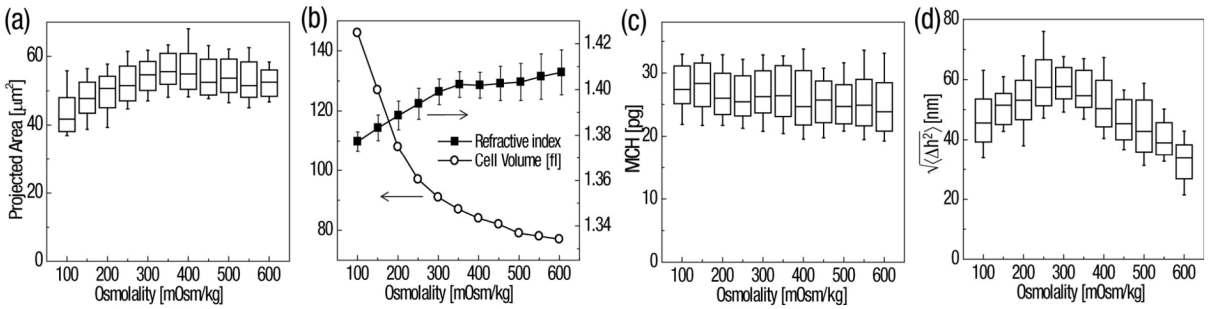

FIG. 2.

(a) Projected areas of RBCs at different osmolalities. (b) Averaged refractive index of RBC cytoplasm (closed symbols) and RBC volume calibrated from Ref. [25] (open symbols). (c) MCHs at different osmolalities. (d) RMS fluctuations in RBC membrane. Each box represents standard deviation for 20 RBCs, center line for median and whisker for min-max data.

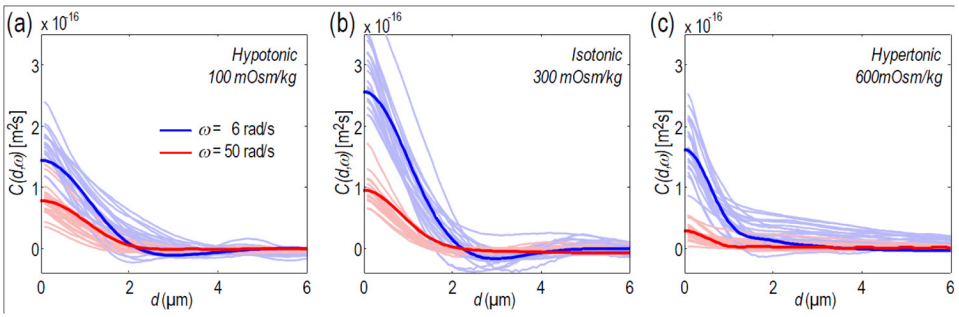

FIG. 3.

(a–c), Height-height correlation of RBC membrane fluctuations as a function of projected distance, in hypotonic (a), isotonic (b), and hypertonic (c) solutions. The faint lines are the experimental data for individual RBCs (N=20 per each group), while the thick lines are the theoretical curves using the averaged fitting parameters.

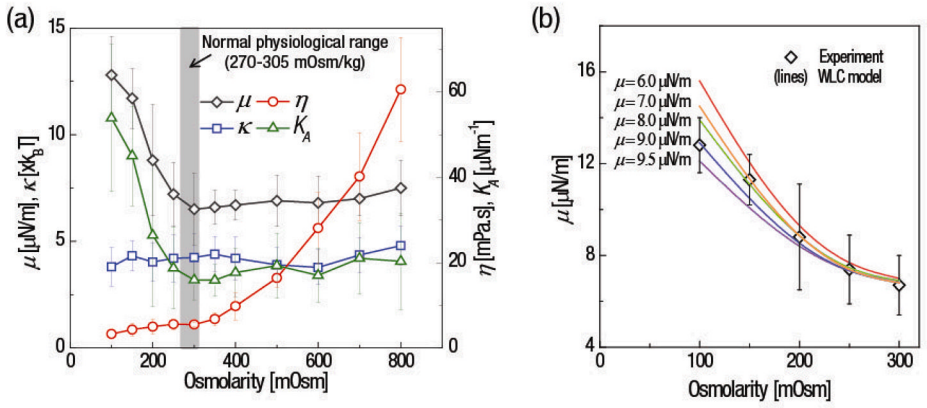

FIG. 4.

(a) Shear modulus μ, cytosol viscosity η_c, and bending modulus κ versus different osmotic pressure. Error bar represents standard deviation for 20 RBCs. (b) The observed increase in μ of the membrane (symbols) compared to WLC predictions for the nonlinear increase in μ associated with the tensing of the membrane (line). Contour lengths used for WLC model are 180 nm, 173 nm, 167 nm, 163 nm, and 167 nm, for μ = 6 μN/m, 7 μN/m, 8 μN/m, 9 μN/m, and 9.5nm μN/m, respectively.